

# On the use of photometer data to map dynamics of the magnetotail current sheet during substorm growth phase

J. A. Wanliss, J. C. Samson, and E. Friedrich

Department of Physics, University of Alberta, Edmonton, Alberta, Canada

**Abstract.** The Canadian Auroral Network for the OPEN Program Unified Study (CANOPUS) is a large-scale ground-based instrument array of remote sensing equipment monitoring the high-latitude ionosphere from the north central to the northwest portion of North America. It provides realtime coverage of auroral events such as magnetospheric substorms. In this paper the variation of magnetotail thickness is estimated during substorm growth phase by using a simple magnetic field model and data from the meridian scanning photometers in the CANOPUS array. An important parameter in the modeling process is the  $\kappa$  parameter, defined as the square root of the minimum curvature radius to maximum Larmor radius ratio. Through use of this parameter we are able to grossly determine the expected proton precipitation regions in the ionosphere. Two examples presented (February 9, 1995, and March 9, 1995) show that crosstail current sheet thinning from 2-0.1  $R_E$  can occur during the course of a growth phase. Within the framework of our model it is demonstrated that the magnetotail field line stretching, associated with thinning of the current sheet, is correlated with the equatorward motion of  $H_\beta$  auroral emissions. Also demonstrated is the Earthward movement of the inner edge of the plasma sheet to within 6  $R_E$ .

## 1. Introduction

The magnetotail current sheet plays a crucial role in magnetospheric substorm dynamics. One way to try to study the magnetotail current sheet begins in the ionosphere, since magnetic field lines that thread the current sheet eventually close in the ionosphere. Differing views of the ionosphere are obtained by unlike, but complementary, ground-based instruments such as radars, magnetometers, and optical measurements. Such ground-based instruments allow the space physicist to acquire an almost instantaneous picture of the two-dimensional distribution of ionospheric currents, plasma flow, particle precipitation, and auroral luminosity over a large portion of the polar ionosphere. One such collection of instruments is the Canadian Auroral Network for the OPEN Program Unified Study (CANOPUS); a large-scale array of remote-sensing equipment monitoring the high-latitude ionosphere from the north central to the northwest portion of North America. CANOPUS includes an array of four meridian scanning photometers (MSP) [Rostoker *et al.*, 1995] which are capable of scanning auroral emissions at various wavelengths.

With the MSP, one can monitor key auroral wavelengths that provide information useful, for example,

in identifying the locale of specific auroral activations. The importance of these tools is appreciated as one considers that any region of the magnetosphere maps to the ionosphere along magnetic field lines. Such a mapping means that knowledge of where the particles and currents are in the ionosphere can give information about the state of the magnetosphere. For example, Samson *et al.* [1992] and Samson [1994] used CANOPUS MSP and low-altitude satellite measurements to demonstrate that substorm expansive phase intensification starts near the Earth, at no more than 8-10  $R_E$ .

While the ground-based coverage of auroral activity in the ionosphere is quite good, satellite measurements of substorm activity in the magnetosphere give at best only a few point measurements. Therefore to make the connection from the ionosphere to the magnetosphere, one must resort to a magnetic field model to map from one region to the other. Among the most popular magnetic field models are the time-independent models of Tsyganenko [1987, 1989, 1995, 1996] (hereafter referred to as T87, T89, T95, T96, respectively). These global models are based on statistical analysis of years of satellite observations.

Since the Tsyganenko models are statistical fits compiled from data measured over all phases of magnetic activity, one cannot expect them to accurately represent the current sheet region during substorms, especially when the crosstail current is very thin. An empirical model tends to have a thicker current sheet than is present in the real magnetotail since the real mag-

netotail may move up and down in the  $Z$  direction. Such tail “flapping” broadens the apparent observed thickness obtained by averaging or binning the satellite data. *Fairfield* [1991] evaluated the T87 model using a large number of *in situ* measurements of the magnetic field. One of his conclusions was that the model is not stretched enough in the near-earth region, a consequence of a too thick current sheet.

*Kaufmann* [1987] was the first to show that a requirement of growth phase was enhanced stretching of field lines, particularly in the near-tail region. More recently, *Pulkkinen et al.* [1991, 1992, 1994, 1998] developed a time-dependent model of the growth phase based on T89. In their studies, Pulkkinen et al. had to modify T89 to include a localized thinning of the crosstail current sheet so that the stretching of the near-Earth magnetic field during the substorm growth phase was reasonable. Similarly, *Lu et al.* [1999] modified T96 by incorporating an adjustment to the intensity and thickness of the near-tail current sheet and a contribution from the substorm current wedge.

In this paper we use the distribution of auroral luminosity (from MSP data) to gain information about the nature and location of the magnetotail source regions of the precipitating ions. We wish to clarify and quantify the nature of the relationship of the equatorward motion of the optical emissions to the stretching of field lines during the substorm growth phase and the initial poleward motion at substorm intensification associated with dipolarization. To the best of our knowledge this relationship has only been stated but never demonstrated quantitatively. Instead of using the more complicated models mentioned above, we introduce a simple magnetic field model and use it to find the temporal variations in the thickness of the magnetotail current sheet, and the location of the inner edge of the plasma sheet, during the substorm growth phase.

## 2. Proton Precipitation in the Auroral Ionosphere

CANOPUS MSPs are excellent tools for investigating the precipitation of charged particles in the auroral ionosphere, including intervals with very active substorm processes. When electrons and protons precipitate into the auroral oval, they collide with ionospheric particles, leaving these in excited states. De-excitation of these atmospheric particles is the main cause of auroral luminosity. We will now address the question of where these precipitating electrons and protons come from.

In the Earth’s magnetotail, particles sometimes do not conserve the first adiabatic invariant due to significant magnetic field variations on the scale of the particle gyroradius. The  $\kappa$  parameter, defined by *Büchner and Zelenyi* [1987], is useful in characterizing the nonadiabatic particle behavior. The parameter is defined by

$$\kappa = \sqrt{\frac{R}{\rho}}, \quad (1)$$

where  $R$  is the magnetic field line radius of curvature and  $\rho$  is the particle gyroradius measured in the current sheet. The dependencies in the  $\kappa$  parameter show that the type of particle motion (namely adiabatic and chaotic) is dependent on both the magnetic field geometry and particle energy. Magnetotail models have strongly curved field lines and the magnetic field component normal to the current sheet can become very small. When the radius of curvature of the magnetic field at the current sheet becomes comparable to the particle gyroradius, the particle is pitch angle scattered. In the distant tail  $\kappa \ll 1$ . *Ashour-Abdalla et al.* [1994] showed that meandering motion in this regime can lead to the formation of a thin current sheet. However, close to the Earth where the dipole field is stronger,  $\kappa$  can be much larger than unity, and the particle motion is adiabatic. In between, at the transition between taillike and dipolelike field configurations, plasma sheet ions can have variable  $\kappa$  values. *Zelenyi et al.* [1990] demonstrated that for  $1 \leq \kappa \leq 3$  near-earth plasma sheet ions may become untrapped. For  $\kappa \ll 1$ , the situation reverts to a more generalized adiabaticity [*Sonnerup*, 1971], and the protons execute a meandering motion about the current sheet [*Speiser*, 1965]. *Delcourt et al.* [1996] recently showed that ions corresponding to  $\kappa$  values between 1 and 3 can be pitch angle scattered out of the current sheet, a fraction of which may enter the loss cone and precipitate into the ionosphere. If the magnetic field is very stretched, the fraction entering the loss cone can be quite significant [*Lyons and Speiser*, 1982]. *Liu et al.* [1998] quantified this effect using theoretical models of a stretched near-Earth current sheet.

One may use a magnetic field model to map auroral luminosity from the ionosphere to the magnetosphere. This is done by locating the luminosity region of interest and then following the magnetic field line that threads this region to its position in the current sheet. What we propose to do is just the opposite, a mapping from the magnetotail to the ionosphere. First we locate positions in the magnetotail where pitch angle scattering of protons can be very important (i.e.,  $1 \leq \kappa \leq 3$ ). Then we map these regions to the ionosphere, where we assume they correspond to proton auroral precipitation. Ideally, this mapping would correspond to the real luminosity, measured by the MSP. However, the mapping problem depends on numerous independent parameters that we do not know accurately. For example, the  $\kappa$  parameter is sensitive to particle energy, current sheet thickness, and the normal component of the magnetic field in the crosstail current sheet region. We will use the 486.1 nm ( $H_\beta$ ) auroral emissions measured by the MSP for our study, for which the energy of the precipitating protons, based on a comparison of data from the DMSP satellite and CANOPUS  $H_\beta$ , is several to tens of keV, with an average of  $\sim 20$  keV [*Samson et al.*, 1992]. We will use a simple magnetic field model and vary only the parameter related to the crosstail current sheet half-thickness ( $L_z$ ). In this way we will be able to determine how sensitively the proton precipitation depends on this model current sheet thickness during

the course of the growth phase. *Samson et al.* [1992] showed that the 486.1 nm ( $H_\beta$ ) emissions can be used to delineate the Earthward edge of the plasma sheet. Thus, in addition to the current sheet thickness, we may derive the position of the inner edge of the plasma sheet from the equatorward edge of the  $H_\beta$  emissions.

### 3. Magnetic Field Model

Our magnetotail model attempts to approximate the topology of the magnetotail during the substorm growth phase. Accordingly, we use established aspects of the growth phase to define the model. It is worthwhile to repeat salient features of the growth phase currents and fields. First of all, during a substorm growth phase, the near-Earth crosstail current can thin to fractions of an  $R_E$  [*Sergeev et al.*, 1993; *Sanny et al.*, 1994; *Kubyshkina et al.*, 1999]. At the same time the crosstail current intensifies in the near-Earth region [*Kaufmann*, 1987]. The current intensification is restricted in radial extent and azimuthally to within a few hours around magnetic midnight [*Baker and McPherron*, 1990; *Ijima et al.*, 1993; *Baker et al.*, 1993]. These changes in the crosstail current result in the magnetic field becoming very weak and taillike in the midplane [*Kokubun and McPherron*, 1981; *Pulkkinen et al.*, 1992; *Nakai et al.*, 1997] and lead to a localized region of weak magnetic field near the neutral sheet. As well, these changes in current sheet structure are expected to lead to enhanced ionospheric precipitation.

Instead of modifying the multiparameter Tsyganenko models, we have elected to use a simpler magnetic field model that has fewer components. As mentioned before, the Tsyganenko models calculate a statistical crosstail current that represents an average over all configurations of the magnetosphere. There is good reason therefore to expect that these models do not adequately fit substorm growth phase, when the magnetotail is very stretched and extremely thin current sheets are known to exist. Modifications that are required to fit these models to growth phase bear out this conviction [*Pulkkinen et al.*, 1991, 1992, 1994, 1998; *Lu et al.*, 1999]. Our model has the advantage of simplicity, thus making it easy to understand the dynamics of the current sheet during the growth phase. The model comprises a dipole field, an equilibrium tail component, and an azimuthally and radially confined weak magnetic field region (WFR). All three modular components, expressed in dipole coordinates, are used to build up the final model configuration

$$\vec{B}(\vec{r}) = \vec{B}^{\text{Dipole}}(\vec{r}) + \vec{B}^{\text{Tail}}(\vec{r}) + \vec{B}^{\text{WFR}}(\vec{r}). \quad (2)$$

For the tail component we use the *Zwingmann* [1983] two-dimensional equilibrium model, given by

$$\begin{aligned} B_x^{\text{Tail}} &= B_0 F(x) \tanh(F(x) \frac{z}{L_z}) \\ B_y^{\text{Tail}} &= 0 \end{aligned} \quad (3)$$

$$B_z^{\text{Tail}} = B_0 L_z \frac{\partial_x F(x)}{F(x)} [1 - F(x) \frac{z}{L_z} \tanh(F(x) \frac{z}{L_z})],$$

where the following values were chosen for the various parameters; the lobe magnetic field  $B_0 = 50$  nT and  $L_z$  is the magnetotail current sheet half-thickness. The function  $F(x)$  is slowly varying in the parameter  $x$ .  $F(x)$  decreases with distance from the Earth and is chosen as

$$F(x) = (1 - \frac{\epsilon x}{L_z \nu})^{-\nu}. \quad (4)$$

A detailed description of the parameters introduced is given by *Zwingmann* [1983]. The parameters  $\nu=1.25$  and  $\epsilon=0.002$  relate to how fast the lobe field falls off with downtail distance.

The final component to the model is a three-dimensional magnetic structure that creates a depression, or WFR, near the Earth. The magnetic field is given by

$$\begin{aligned} B_x^{\text{WFR}} &= 0 \\ B_y^{\text{WFR}} &= B_p L_y \text{sech}(\frac{x+10}{L_y}) \tanh(\frac{y}{L_y}) \partial_z G(z) \\ B_z^{\text{WFR}} &= B_n - B_p \text{sech}(\frac{x+10}{L_y}) \text{sech}^2(\frac{y}{L_y}) G(z), \end{aligned} \quad (5)$$

where the background normal field in the distant current sheet is  $B_n = 1$  nT. The parameter  $B_p = 28.45$  nT causes a depression in the magnetic field near the current sheet region, and  $L_y = 3^{1/2} R_E$  determines how wide the depression is in the current sheet region. Finally, the function  $G(z)$ , given by

$$G(z) = (1 + \frac{z^2}{L_y^2})^{-1/3}, \quad (6)$$

constrains the depression of the magnetic field to be confined primarily to the current sheet region around  $Z=0$ . The WFR is so named because it creates a depression in the magnetic field around  $X = -10 R_E$ . It is constructed to simulate the observation, mentioned at the start of this section, that the growth phase current sheet is enhanced in a radially and azimuthally confined region. Its effect is to cause enhanced stretching of magnetic field lines in the near-Earth region. Furthermore, various theoretical models predict a region of small  $B_z$  will form in the intermediate region between dipolelike and taillike magnetic fields under the action of a dawn-to-dusk electric field [*Erickson*, 1984; *Hau et al.*, 1989]. As well, observational studies have demonstrated that a region of depressed magnetic field occurs in the near-Earth during the growth phase [*Lui et al.*, 1992; *Sergeev et al.*, 1993]. The chosen position for the WFR, namely about  $X = -10 R_E$ , is justified below in terms of observational data. The model NS magnetic field is not a fit to the observational data presented. Rather, the comparison of the model with observational data is intended to demonstrate that the model is not unreasonable.

In the study by *Rostoker and Skone* [1993], AMPTE, ISEE, and IMP 8 data were selected at times when clear neutral sheet crossings were taking place. Using these data they constructed an analytical representation of  $B_z$  as a function of downtail position. In Figure 1, magnetic field values in the neutral sheet are compared for the new model and the empirical function of *Rostoker and Skone* [1993] (solid line), as well as other statistical observations of neutral sheet magnetic field. The model field is a reasonable fit of the *Rostoker and Skone* function in the regions tailward of  $\sim 14 R_E$ . Near  $X = -11 R_E$ , which is the intermediate region between dipolelike and taillike magnetic fields, the new magnetic field model has a depression not found in that statistical model and is larger within geostationary orbit. As with T96, the statistical model of *Rostoker and Skone* will tend to average out the extremes of magnetic field behavior, so not too much importance should be placed on this discrepancy. This is especially so in light of experimental observations of regions of small normal magnetic field during times when the magnetotail geometry is stretched [*Lui et al.*, 1992; *Sergeev et al.*, 1993].

Also included in this figure are the statistical observations of *Nakai et al.* [1997] representing equatorial  $B_z$  during quiet and disturbed conditions. These data show that during quiet times the magnetic field is larger than

the *Rostoker and Skone* [1993] curve, whereas for disturbed times, these data are smaller in the near-Earth but larger beyond geostationary orbit. Within the standard deviations of these data (not shown) their results are the same as *Rostoker and Skone*. The equatorial  $B_z$  data from *Lui et al.* [1992] (squares) and *Sergeev et al.* [1993] (star) are the most useful, for they were specifically measured during case studies of the growth phase and are in much better agreement with the new model in the intermediate region between dipolelike and taillike magnetic fields. These data show that during the growth phase, regions of small normal magnetic field ( $B_z$ ) can occur in the near-Earth. The minimum in the model magnetic field is located around  $X = -11 R_E$ .

*Kaufmann* [1987] showed that a requirement of growth phase was enhanced stretching of field lines, particularly in the near-tail region. He achieved the requisite taillike field configuration at  $\sim 6.6 R_E$  by using a field model comprising a dipole field and a system of three infinitely thin current sheets in the tail. Our model is slightly more complex and reproduces similar field geometries. Figure 2 shows magnetic field lines for thick ( $L_z = 1 R_E$ ) (Figure 2a) and thin ( $L_z = 0.05 R_E$ ) (Figure 2b) crosstail current sheet half-thickness parameter. Thinning of the current sheet is evidenced by the decreased magnetic field radius of curvature in Figure 2b.

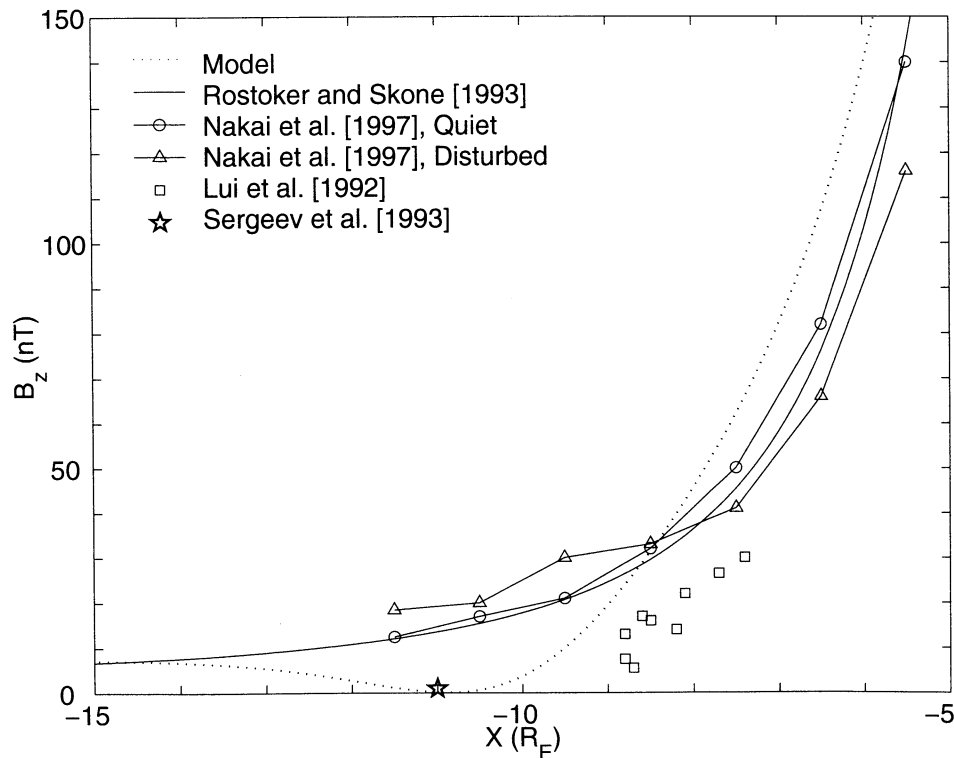


**Figure 1.** Model magnetic field values in the neutral sheet compared to various satellite measurements. The dotted line indicates the model magnetic field; the solid line is the empirical function of *Rostoker and Skone* [1993], calculated irrespective of substorm phase. The circles and triangles indicate  $B_z$  during disturbed and quiet periods from the measurements of *Nakai et al.* [1997]. The squares are the values from *Lui et al.* [1992], measured just prior to the onset of magnetic field dipolarisation; the single star is for the growth phase measurements at  $X = -11 R_E$  by *Sergeev et al.* [1993].

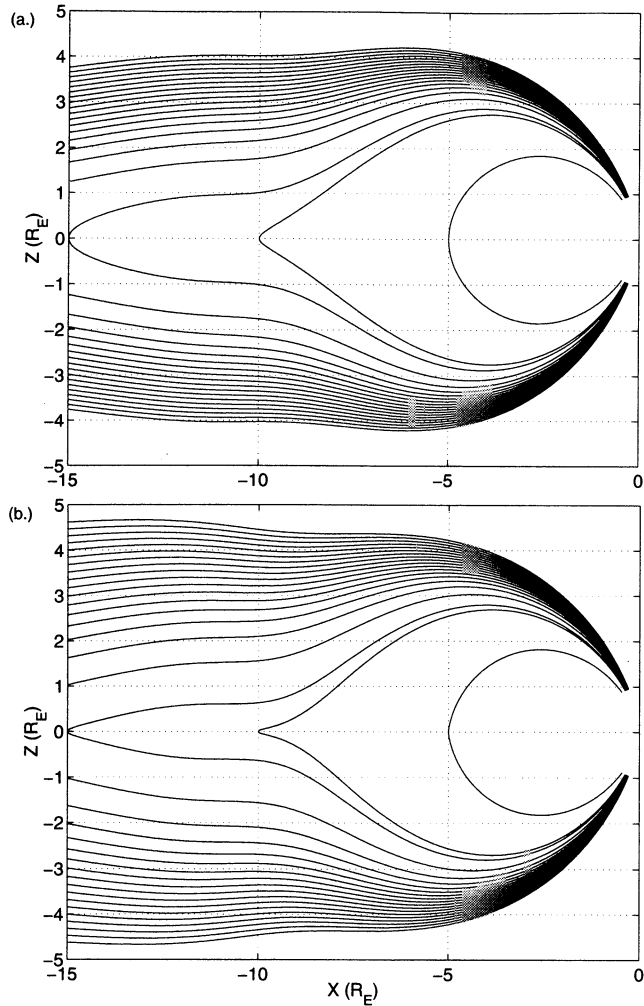


**Figure 2.** Model magnetic streamlines in the noon-midnight meridian for current sheet half-thickness (a)  $L_z = 1 R_E$  and (b)  $L_z = 0.05 R_E$ . In the latter case the thinner current sheet is evidenced by the decreased magnetic field line radius of curvature.

These two figures are similar to *Kaufmann* [1987, Figures 2 and 3] and include the negative curvature in the near-Earth magnetic field lines.

#### 4. Modeling Technique

The magnetic field model may be used to predict where in the ionosphere regions of auroral proton precipitation will occur. In light of the observational constraints for  $H_\beta$  we choose proton energies of 10, 20, and 30 keV to calculate the  $\kappa$  parameter in the crosstail current sheet. These energies for precipitating protons are around the average reported by *Samson et al.* [1992]. Next the parameter  $L_z$ , which is related to the model current sheet thickness, is varied, and the  $\kappa$  parameter is calculated as a function of  $L_z$  and the allowed energy ranges (namely 10-30 keV). The position and depth of the magnetic WFR is not varied during the fitting procedure. Near the Earth the  $\kappa$  parameter is largest, and

it decreases with distance downtail. The boundary between adiabatic and nonadiabatic particle motion is defined by the  $\kappa = 3$  separatrix in the near-earth neutral sheet. As the current sheet thins, the location of the equatorward border of proton precipitation, defined by this separatrix, moves earthward. *Samson et al.* [1992] found that the onset of the substorm intensification occurs in the region of proton precipitation which maps to the inner edge of the plasma sheet, namely the  $\kappa = 3$  separatrix. In the least squares fitting procedure, we will assume that the  $\kappa = 1$  boundary, defined from the 10-30 keV protons, corresponds to the poleward border of  $H_\beta$  emissions, although this may not always be true. Figure 3 shows the model predicted latitudes of auroral  $H_\beta$  emissions, plotted against current sheet thickness parameter,  $L_z$  (cf. equation (3)). The borders for the 10 keV protons are shown as dot-dashed lines, 20 keV are solid lines, and 30 keV are dotted lines. In all cases it is clear that as the current sheet thins, the precipitation region moves equatorward. As well, the equatorward border of the precipitation region moves equatorward at a faster rate for small current sheet thicknesses.

In order to fit the model data to the MSP emissions, we required a time series of the poleward and equatorward borders of the  $H_\beta$  luminosity. These were obtained by fitting the emission borders to a Gaussian function. Where it was not possible to get a good fit using the Gaussian, we adopted a step function fit [*Blanchard et al.*, 1995, 1997]. Finally, we will use least squares fitting of these model data to the actual MSP measurements to see how well the model predicts the observed locations of the auroral regions of luminosity.

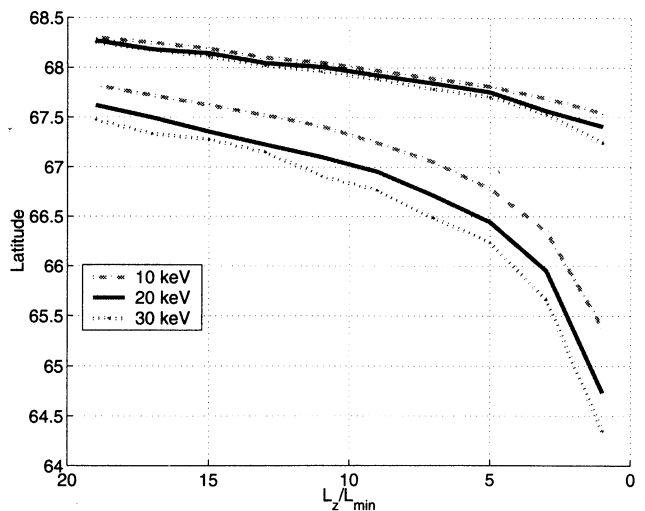


**Figure 3.** Model predictions for the regions of proton precipitation in the ionosphere. Precipitation occurs in the region between the high- and low-latitude borders. The ordinate is invariant latitude in degrees, and the abscissa is the model current sheet half-thickness, normalised to  $L_{\min} = 0.05 R_E$ . These curves were computed by calculating the regions in the magnetotail where 10, 20, and 30 keV protons achieve  $1 \leq \kappa \leq 3$ , and then mapping these regions to the ionosphere  $\kappa$  is defined in equation (1)

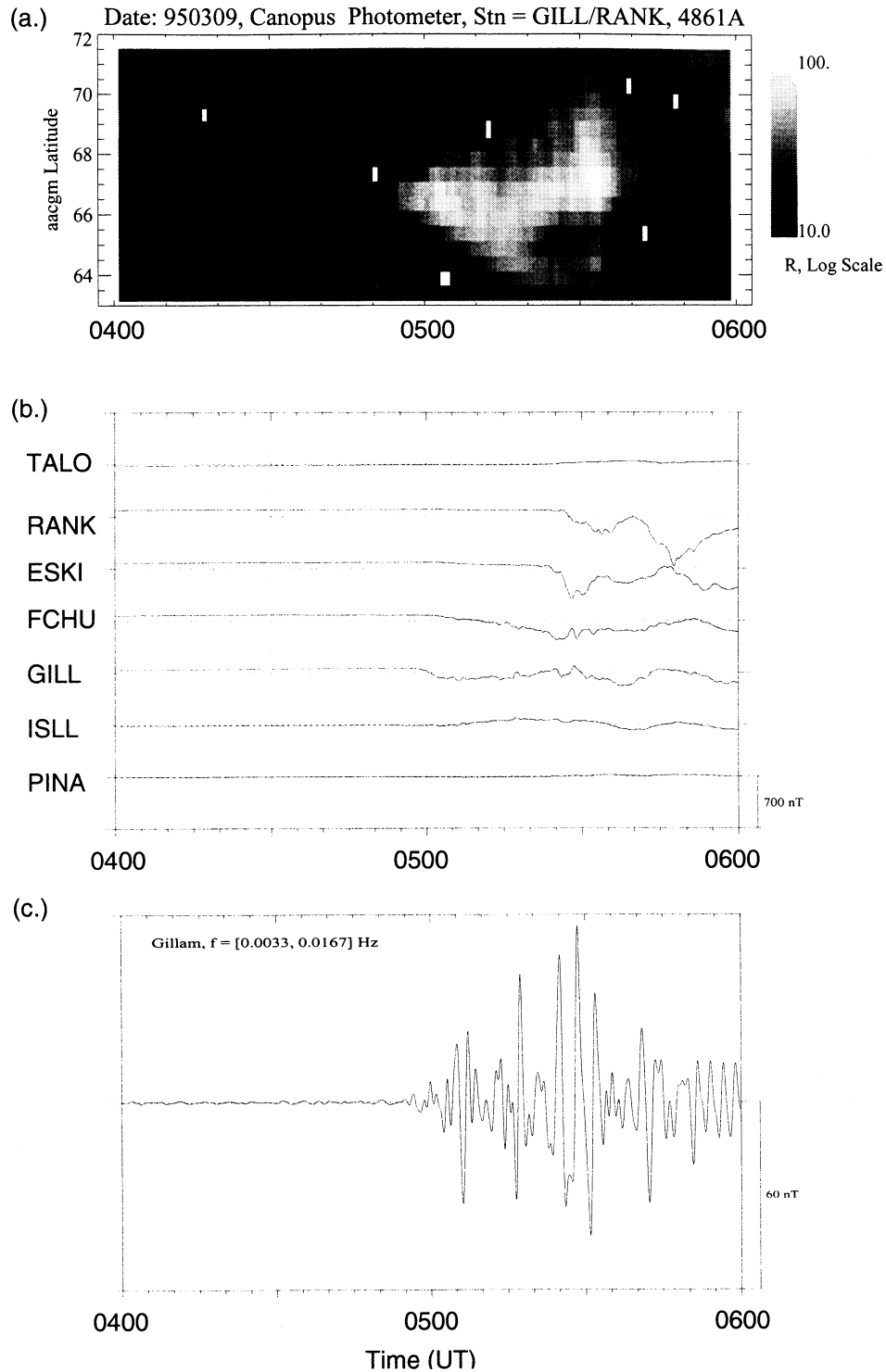


**Figure 4.** (a) Meridian scanning photometer data (486.1 nm) from Rankin Inlet and Gillam stations in the CANOPUS array showing the growth phase and intensification of a substorm event on March 9, 1995. AACGM coordinates are explained by *Baker and Wing* [1989]. (b) Magnetic  $X$  component from the Churchill line of magnetometers. (c) Magnetic  $X$  component Pi2 pulsations at Gillam. Local magnetic time is approximately UT minus 6 hours for the Churchill line.

## 5. Case Studies

As discussed in section 4, the magnetic field model can be used to connect magnetically the field and current variations in the magnetotail to the changes in the precipitation pattern seen in the auroral regions. We studied several events for which the growth phase is very clear and has no Pi2 pulsations before the expansive phase onset. In this section, data from two representative sample substorm events are presented.

### 5.1 March 9, 1995

For the substorm on March 9, 1995, we looked at the interval 0400-0600 UT. *Voronkov et al.* [1999] studied this event in detail and estimated that growth phase commences between 0325-0335 UT. In Figure 4a we show the  $H_\beta$  (486.1 nm) emissions for 0400-0600 UT. The data are in the form of emission intensity versus invariant latitude and time, and have a 1 minute temporal resolution. At 0400 UT, preexisting proton aurora were moving slowly equatorward ( $\sim 0.5^\circ/10$  min), and the equatorward motion increased rapidly after  $\sim 0430$  UT ( $\sim 1^\circ/10$  min). Figure 4b presents the simultaneous magnetometer data from the Churchill line of magnetometer stations. Only the geomagnetic north-south ( $X$ ) component is shown. A positive perturbation of the magnetic  $X$  component appeared after  $\sim 0400$  UT, which indicates an enhancement in the eastward electrojet. The perturbation grew in magnitude until the expansive phase onset began at 0459 UT. Figure 4c shows the impulsive Pi2 pulsations obtained by filtering the raw data from the Gillam station. No Pi2 pulsations are present prior to expansive phase onset at 0459 UT, indicating a “quiet” growth phase. Figure 5 shows the simultaneous 630.0 nm red emissions from low energy precipitating electrons ( $< 1$  keV). The poleward border of these emissions define the high-latitude plasma sheet boundary [Blanchard *et al.*, 1995]. The latitudinal ex-

tent of these emissions, indicated by arrows, can be used to estimate the plasma sheet thickness. We will present these results for plasma sheet thickness in a later paper. For now we will concentrate only on the  $H_\beta$  and consider only the crosstail current sheet thickness.

Figure 6a shows the  $H_\beta$  poleward and equatorward borders obtained in the previously described method. These borders are calculated during the late growth phase and early expansive phase between 0430-0510 UT. Error bars are included which are approximately equal to the latitudinal resolution of the photometer observations. The model best fit predictions are shown as circles. From these fits to the luminosity borders, we obtained estimates for the model current sheet thickness during the late growth and early expansive phases. The thicknesses quoted here are calculated at  $X = -8 R_E$ . The solid line in Figure 6b (right-hand ordinate) indicates the location of the model plasma sheet inner edge. According to the model calculations, the plasma sheet inner edge moved towards the Earth, and at the time of the substorm intensification it was inside  $6 R_E$ . The line marked with circles in Figure 6b is the best fit current sheet thickness, calculated at  $8 R_E$ . At the start of the modeling interval, at 0430 UT, the current sheet was almost  $2 R_E$  thick. It rapidly decreased, and within 20 min was  $0.2 R_E$  thick. This is consistent with satellite measurements [Fairfield, 1984; Mitchell *et al.*, 1990; Sergeev *et al.*, 1993].

Next we calculated the current sheet thickness as a function of time. We performed a least squares fit for an exponential function between 0430-0510 UT, expressed in terms of the current sheet half-thickness,  $L_z$ , as

$$L_z(t) = L_0 \exp(-t/\tau), \quad (7)$$

where  $L_0 = 0.89 R_E$  and the timescale  $\tau = 9.6$  min.

It is noteworthy that there is a high degree of correlation between the thinning of the current sheet, cor-

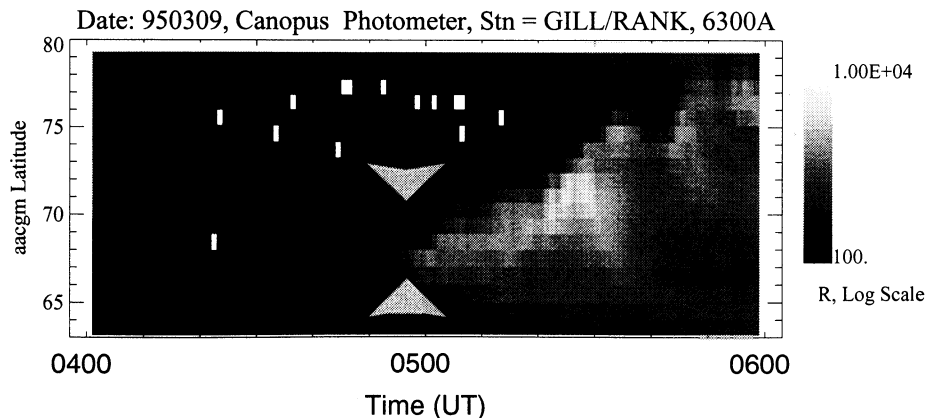


**Figure 5.** Meridian scanning photometer data (630.0 nm) from Rankin Inlet and Gillam stations in the CANOPUS array showing the growth phase and intensification of a substorm event on March 9, 1995. AACGM coordinates are explained by *Baker and Wing* [1989]. The arrows indicate the latitudinal extent of the emissions at expansive phase onset. The poleward border of luminosity defines the high-latitude plasma sheet boundary.

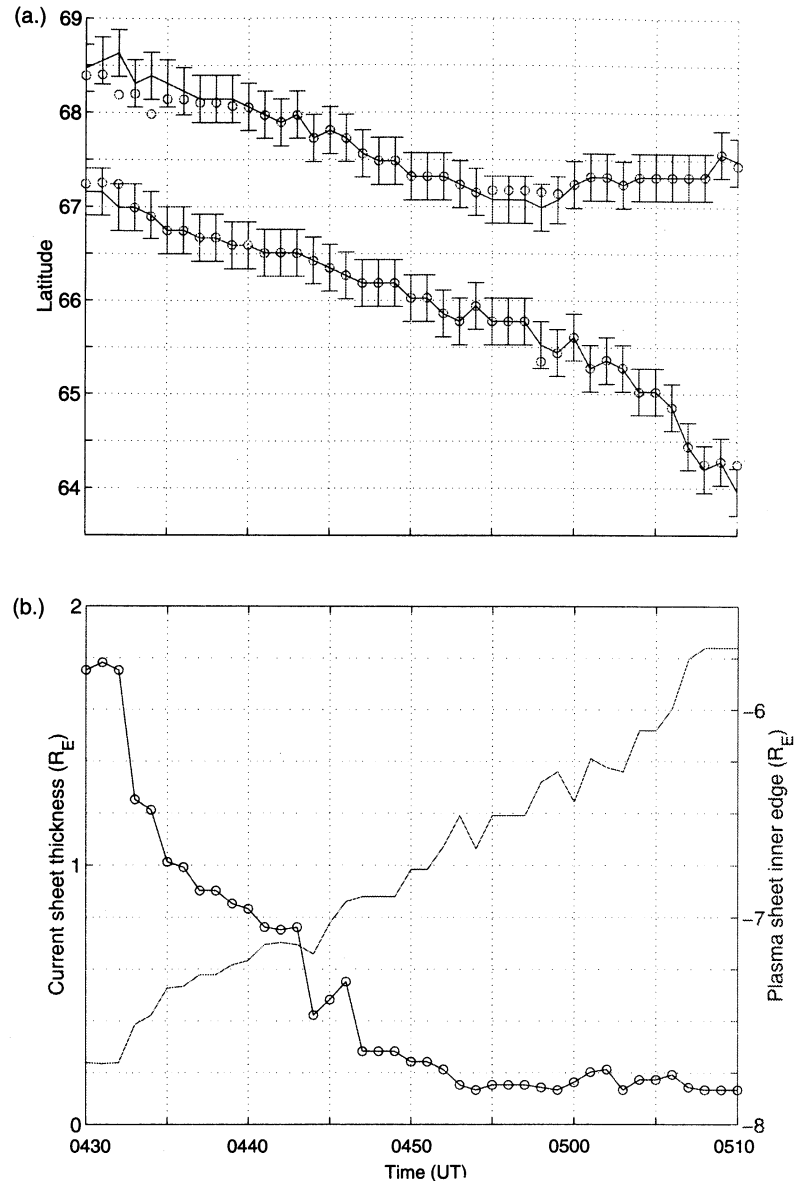


**Figure 6.** (a) March 9, 1995,  $H_\beta$  emission boundaries are shown by the solid line with error bars. The best fit values, calculated from the magnetic model predicted precipitation regions, are indicated by circles. (b) Model predictions for the current sheet thickness at  $8 R_E$  (left ordinate), and plasma sheet inner edge position (right ordinate).

responding to magnetic field line stretching, and the equatorward motion of the proton aurora. Within the framework of our model, this implies that the equatorward motion of auroral precipitation is directly related to the stretching of the magnetic field lines in the magnetotail. To our knowledge, this is the first time this has been quantitatively demonstrated.

## 5.2 February 9, 1995

This substorm has been extensively studied [Lui *et al.*, 1998]. Owing to an unusually long northward interplanetary magnetic field, the magnetosphere was as close to a low energy or “quiet” state as is likely possible before a substorm. Figure 7a shows the  $H_\beta$  emissions

from 0330-0530 UT. Growth phase began at  $\sim 0335$  UT, as seen in enhanced  $H_\beta$  emissions and the magnetometer data. From this time the  $H_\beta$  emissions continued moving equatorward until the expansive phase onset at 0437 UT, at which time the emissions rapidly moved poleward. Figure 7b shows the ground magnetometer  $X$  component at various locations in the Churchill line. Figure 7c shows the Pi2 pulsations obtained by filtering the raw data from the Back station and demonstrates that prior to the expansive phase onset no Pi2 pulsations were visible.

The best least squares fit of the model precipitation regions to the emission borders, calculated between 0400-0440 UT, are shown in Figure 8a. The best fit only

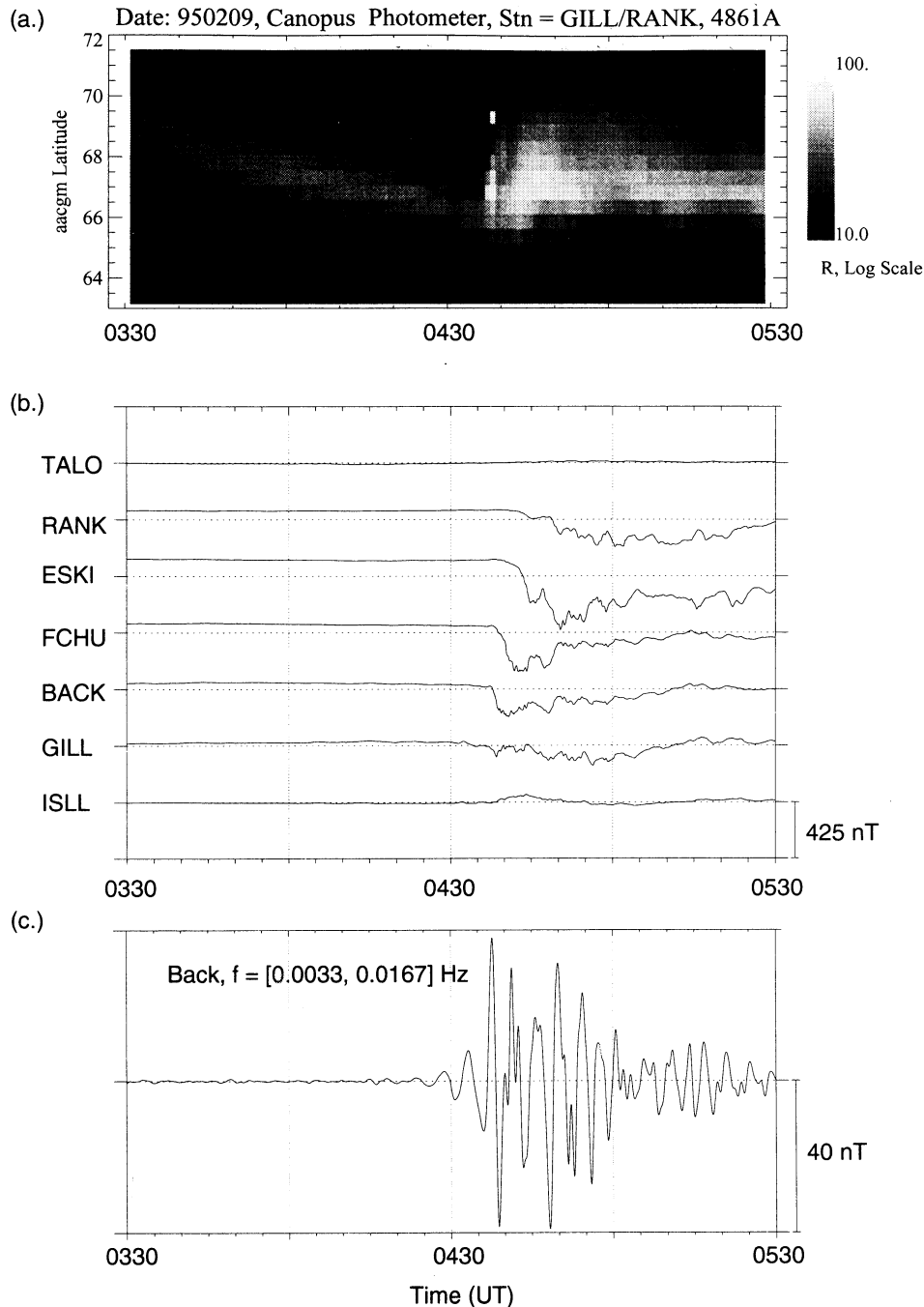


**Figure 7.** (a) Meridian scanning photometer data (486.1 nm) from Rankin Inlet and Gillam stations in the CANOPUS array showing the growth phase and intensification of a substorm even on February 9, 1995. AACGM coordinates are explained by *Baker and Wing* [1989]. (b) Magnetic  $X$  component from the Churchill line of magnetometers. (c) Magnetic  $X$  component  $\text{Pi}2$  pulsations at Fort Churchill. Local magnetic time is approximately UT minus 6 hours.

appears to be reasonable up to  $\sim 0428$  UT; after this time the model is not a good fit to the high-latitude precipitation border (Figure 8a). As with the previous example, the model plasma sheet inner edge was driven toward the Earth and was little more than  $6 R_E$  away at intensification. During the early stages of the modeling interval the predicted current sheet thickness is about  $0.7 R_E$ . By 0430 UT it slightly less than  $0.1 R_E$  thick.

An interesting observation is that the current sheet remains extremely thin ( $\sim 0.1 R_E$ ) for tens of minutes prior to the substorm intensification. This observation is helpful in theoretical modeling of growth phase, where current sheet thickness is an important parameter. An exponential fit to the model crosstail current sheet half-thickness yielded  $L_0 = 0.60 R_E$  and  $\tau = 5.2$  min. The exponential fit was calculated between 0402 and 0428

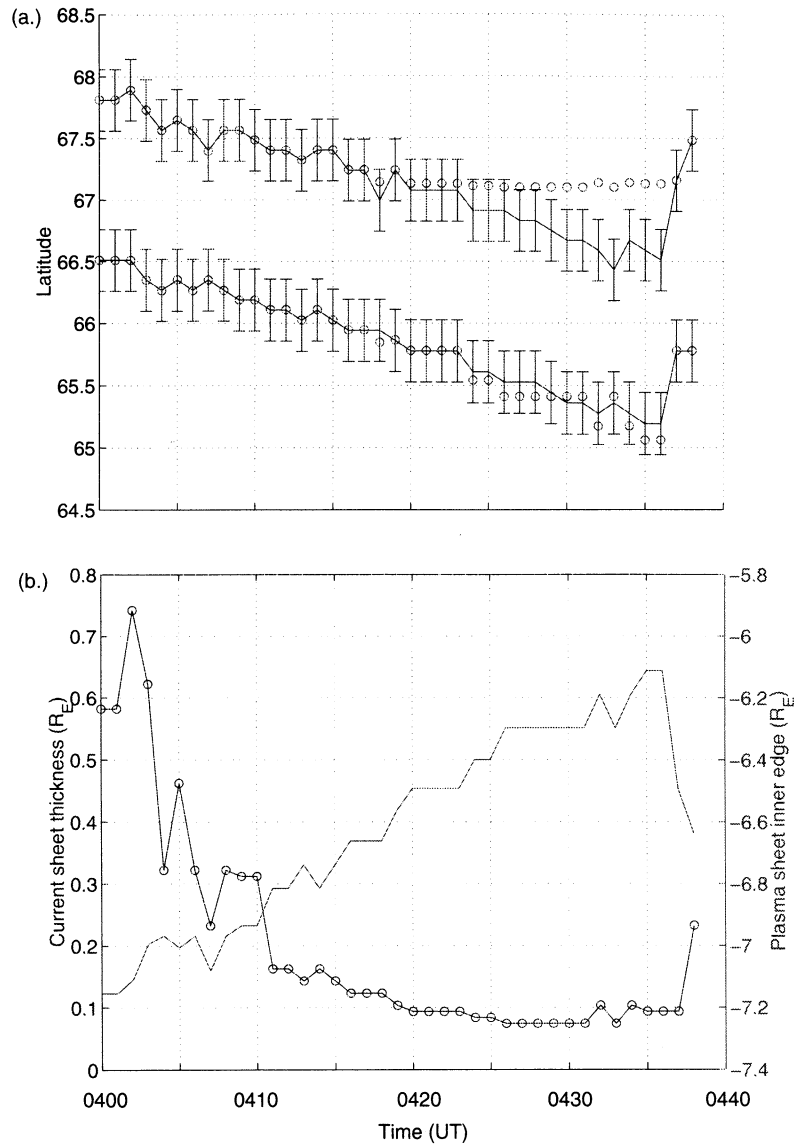


**Figure 8.** (a) February 9, 1995,  $H_\beta$  emission boundaries are shown by the solid line with error bars. The best fit values, calculated from the magnetic model predicted precipitation regions, are indicated by circles. (b) Model predictions for the current sheet thickness (left ordinate) and plasma sheet inner edge position (right ordinate).

UT. In this case, the timescale of growth phase thinning is smaller than that for the March 9, 1995, event. If one assumes that current sheet thickness corresponds inversely to energy input into the magnetosphere, this implies that the rate of energy input was faster than for the March 9, 1995, case. Equatorward motion of the auroral luminosity acts as a proxy to the energy input into the auroral oval. Luminosity regions at higher latitudes imply a less stressed magnetotail configuration. For this situation, less energy input is required than for when the luminosity regions are at low latitudes, and the magnetotail is more stressed. The modeling is corroborated by the MSP data which show that the region of luminosity for February 9 was driven further equatorward than for the March 9 case. Another event studied on February 23, 1995 (data not shown), is consistent

with this hypothesis. For this event (February 23, 1995) we found a timescale of 22.7 min for current sheet thinning, and the luminosity boundaries were consistently poleward of the present data.

For interest, we also show the February 9, 1995, best fit at expansive phase onset (0437 UT). It is fascinating that the model predicts an impulsive thickening of the current sheet and tailward motion of the plasma sheet inner edge. However, not too much confidence should be placed in the model statistics at onset because the magnetotail geometry is changing so rapidly at this time. Future models will address this issue. For each of the events studied we found that the predicted locations of precipitating protons proceed equatorward at the same rate as the  $H_\beta$  auroral luminosity. Again, this provides evidence of the correlation between mag-

netic field line stretching and the equatorward motion of the proton aurora.

## 6. Conclusion

In this report our thesis was that the  $H_\beta$  auroral emissions are partly due to the thinning of the equatorial crosstail current sheet. We have demonstrated a simple technique to calculate the thickness of the crosstail current sheet during the growth phase of a magnetospheric substorm. Two length scales are important in this study, namely, the magnetic field radius of curvature in the equatorial plane and the proton gyroradius. At the start of the substorm the current sheet thickness is typically larger than the proton gyroradius and ions behave adiabatically. As the current sheet thins and becomes of the order of the proton gyroradius, they become nonadiabatic and may be scattered into the ionosphere [Zelenyi et al., 1990]. As shown by Liu et al. [1998], strong nonadiabatic behavior can lead to enhanced proton precipitation leading to  $H_\beta$ . By using the ionospheric data as a proxy for precipitation, we are able to map the changing topology of the magnetotail current sheet during substorm growth phase. Together with the MSP data and a simple magnetic field model, we have shown that the crosstail current sheet does indeed thin during the course of a typical growth phase and that this thinning corresponds to an equatorward motion of the region of precipitating protons. For these case studies we found that the current sheet can thin dramatically during the growth phase, from  $2 R_E$  to as little as  $0.1 R_E$  within 40 min. The current sheet can remain extremely thin for tens of minutes. Furthermore, using the fact that the  $H_\beta$  emissions mark the earthward edge of the plasma sheet, we demonstrated that the model inner edge of the plasma sheet moved several  $R_E$  closer to the Earth during the course of the growth phase. At the end of the growth phase on March 9, 1995, we found that it can be within  $6 R_E$ .

Our results give a time dependent description of the magnetic field change during the substorm growth phase. The model predicts an evolution from a less stretched to a more stretched magnetic geometry during the course of the growth phase and the equatorward motion of the precipitation region. An outstanding problem in substorm physics is the accurate mapping of auroral features to the magnetically connected regions in the magnetotail. Although our magnetic field model does not include more complicated and realistic components, it has the benefit that it is extremely simple and is able to make physically reasonable predictions of crosstail current sheet thickness near midnight. This simplicity allows easy access to understand the variation of the crosstail current sheet thickness during substorm growth phase.

We have shown that the growth phase  $H_\beta$  emissions can be at least partially explained by the precipitation of protons out of the thinning crosstail current sheet. Furthermore, magnetic field line stretching in the magnetotail (i.e., thinning of the current sheet) is correlated

with the equatorward motion of the  $H_\beta$ . Finally, the model has demonstrated that the crosstail current can thin to  $\sim 0.1 R_E$  during the course of the growth phase and that the inner edge of the plasma sheet can move to inside  $6 R_E$  at substorm intensification.

**Acknowledgments.** J.A.W. gratefully wishes to thank Gordon Rostoker for helpful comments and suggestions.

Janet G. Luhmann thanks Patrick T. Newell and Ingrid Sandahl for their assistance in evaluating this paper.

## References

- Ashour-Abdalla, M., L.M. Zelenyi, V. Peromian, and L.R. Richard, Consequences of magnetotail ion dynamics, *J. Geophys. Res.*, *99*, 14,891-14,916, 1994.
- Baker, D.N., and R.L. McPherron, Extreme energetic particle decreases near geostationary orbit: A manifestation of current diversion within the inner plasma sheet, *J. Geophys. Res.*, *95*, 6591-6599, 1990.
- Baker, D.N., T.I. Pulkkinen, R.L. McPherron, J.D. Craven, L.A. Frank, R.D. Elphinstone, J.S. Murphree, J.F. Fennell, R.E. Lopez, and T. Nagai, CDAW-9 analysis of magnetospheric events on May 3, 1996: Event C, *J. Geophys. Res.*, *98*, 3815-3834, 1993.
- Baker, K.B., and S. Wing, A new magnetic coordinate system for conjugate studies at high latitudes, *J. Geophys. Res.*, *94*, 9139-9143, 1989.
- Blanchard, G.T., L.R. Lyons, J.C. Samson, and F.J. Rich, Locating the polar cap boundary from observations of 6300 Å auroral emissions, *J. Geophys. Res.*, *100*, 7855-7862, 1995.
- Blanchard, G.T., L.R. Lyons, and J.C. Samson, Accuracy of using 6300 Å auroral emission to identify the magnetic separatrix on the nightside of the Earth, *J. Geophys. Res.*, *102*, 9697-9703, 1997.
- Büchner, J. and L.M. Zelenyi, Chaotization of the electron motion as the cause of an internal magnetotail instability and the substorm onset, *J. Geophys. Res.*, *92*, 13,456-13,466, 1987.
- Delcourt, D.C., J.-A. Sauvaud, R.F. Martin, and T.E. Moore, On the nonadiabatic precipitation of ions from the near-Earth plasma sheet, *J. Geophys. Res.*, *101*, 17,409-17,418, 1996.
- Erickson, G.M., On the cause of X-line formation in the near-Earth plasma sheet: Results of adiabatic convection in plasma sheet plasma, in *Magnetic Reconnection in Space and Laboratory Plasmas*, *Geophys. Monogr. Ser.*, vol. 30, edited by E.W. Hones Jr., pp. 296-302, AGU, Washington, D.C., 1984.
- Fairfield, D.H., Magnetotail energy storage and the variability of the magnetotail current sheet, in *Magnetic reconnection in Space and Laboratory Plasmas*, *Geophys. Monogr. Ser.*, vol. 30, edited by E.W. Hones Jr., pp. 168-177, AGU, Washington, D.C., 1984.
- Fairfield, D.H., An evaluation of the Tsyganenko magnetic field model, *J. Geophys. Res.*, *96*, 1481-1494, 1991.
- Hau, L.N., R.A. Wolf, G.-H. Voight, and C.C. Wu, Steady state magnetic field configurations for the Earth's magnetotail, *J. Geophys. Res.*, *94*, 1303-1316, 1989.
- Iijima, T. et al., Substorm currents in the equatorial magnetotail, *J. Geophys. Res.*, *98*, 17,283-17,298, 1993.
- Kaufmann, T.G., Substorm currents: Growth phase and onset, *J. Geophys. Res.*, *92*, 7471-7486, 1987.
- Kokubun, S., and R.L. McPherron, Substorm signatures at synchronous altitude, *J. Geophys. Res.*, *86*, 11,265-11,277, 1981.

- Kubyskhina, M.V., V.A. Sergeev, and T.I. Pulkkinen, Hybrid input algorithm: An even-oriented magnetospheric model, *J. Geophys. Res.*, *104*, 24,977-24,994, 1999.
- Liu, W.W., G. Rostoker, and J.C. Samson, Precipitation of hot protons from a stretched near-earth current sheet, *COSPAR Colloquia Series*, vol. 9, pp. 165-175, Elsevier Sci., New York, 1998.
- Lu, G., N.A. Tsyganenko, A.T.Y. Lui, H.J. Singer, T. Nagai, and S. Kokubun, Modeling of time-evolving magnetic fields during substorms, *J. Geophys. Res.*, *104*, 12,327-12,337, 1999.
- Lui, A.T.Y., R.E. Lopez, B.J. Anderson, K. Takahashi, L.J. Zanetti, R.W. McEntire, T.A. Potemra, D.M. Klumpar, E.M. Greene, and R. Strangeway, Current disruptions in the near-Earth neutral sheet region, *J. Geophys. Res.*, *97*, 1461-1480, 1992.
- Lui, A.T.Y., et al., Multipoint study of a substorm on February 9, 1995, *J. Geophys. Res.*, *103*, 17,333-17,344, 1998.
- Lyons, L.R., and T.W. Speiser, Evidence for current sheet acceleration in the geomagnetic tail, *J. Geophys. Res.*, *87*, 2276-2286, 1982.
- McPherron, R.L., A. Nishida, and C.T. Russell, Is near-Earth current sheet thinning the cause of auroral substorm onset?, in *Quantitative Modeling of Magnetosphere-Ionosphere Coupling Processes*, edited by Y. Kamide, pp. 252-257, Kyoto, Japan, 1987.
- Mitchell, D.G., D.J. Williams, C.Y. Huang, L.A. Frank, and C.T. Russell, Current carriers in the near-Earth cross-tail current sheet during substorm growth phase, *Geophys. Res. Lett.*, *17*, 583-586, 1990.
- Nakai, H., Y. Kamide, and C.T. Russell, Statistical nature of the magnetotail current in the near-earth region, *J. Geophys. Res.*, *102*, 9573-9586, 1997.
- Pulkkinen, T.I., et al., Modeling the growth phase of a substorm using the Tsyganenko model and multi-spacecraft observations: CDAW-9, *Geophys. Res. Lett.*, *18*, 1963-1966, 1991.
- Pulkkinen, T.I., D.N. Baker, R.J. Pellinen, J. Büchner, H.E.J. Koskinen, R.E. Lopez, R.L. Dyson, and L.A. Frank, Particle scattering and current sheet stability in the geomagnetic tail during the substorm growth phase, *J. Geophys. Res.*, *97*, 19,283-19,297, 1992.
- Pulkkinen, T.I., D.N. Baker, D.G. Mitchell, R.L. McPherron, C.Y. Huang, and L.A. Frank, Thin current sheets in the magnetotail during substorms: CDAW 6 revisited, *J. Geophys. Res.*, *99*, 5793-5804, 1994.
- Pulkkinen, T.I., D.N. Baker, L.L. Cogger, T. Mukai, and H.J. Singer, Coupling of inner tail and midtail processes, in *Substorms-4*, edited by S. Kokubun and Y. Kamide, pp.749-754, Terra Sci., Tokyo, 1998.
- Rostoker, G., and S. Skone, Magnetic flux mapping considerations in the auroral oval and the Earth's magnetotail, *J. Geophys. Res.*, *98*, 1377-1384, 1993.
- Rostoker, G., et al., CANOPUS - a ground-based instrument array for remote sensing the high latitude ionosphere during the ISTP/GGS program, *Space Sci. Rev.*, *71*, 743-760, 1995.
- Samson, J.C., Mapping substorm intensifications from the ionosphere to the magnetosphere, in *Proceedings of the International Conference on Substorms 2*, edited by J.R. Kan, J.D. Craven, and S.-I. Akasofu, pp.237-243, Univ. Alaska, Fairbanks, 1994.
- Samson, J.C., L.R. Lyons, P.T. Newell, F. Creutzberg, and B. Xu, Proton aurora and substorm intensifications, *Geophys. Res. Lett.*, *19*, 2167-2170, 1992.
- Sanny, J., R.L. McPerron, C.T. Russell, D.N. Baker, T.I. Pulkkinen, and A. Nishida, Growth phase thinning of the near-Earth current sheet during the CDAW 6 substorm, *J. Geophys. Res.*, *99*, 5805-5816, 1994.
- Sergeev V.A., D.G. Mitchell, C.T. Russell, and D.J. Williams, Structure of the tail plasma/current sheet at 11  $R_E$  and its changes in the course of a substorm, *J. Geophys. Res.*, *98*, 17,345-17,366, 1993.
- Sonnerup, B.U.O., Adiabatic particle orbits in a magnetic null sheet, *J. Geophys. Res.*, *76*, 8211-8222, 1971.
- Speiser, T.W., Particle trajectories in model current sheets, 1: Analytical solutions, *J. Geophys. Res.*, *70*, 4219-4226, 1965.
- Tsyganenko, N.A., Global quantitative models of the geomagnetic field in the cislunar magnetosphere for different disturbance levels, *Planet. Space Sci.*, *35*, 1347-1358, 1987.
- Tsyganenko, N.A., A magnetospheric magnetic field model with a warped tail current sheet, *Planet. Space Sci.*, *37*, 5-20, 1989.
- Tsyganenko, N.A., Modeling the earth's magnetospheric magnetic field confined within a realistic magnetopause, *J. Geophys. Res.*, *100*, 5599-5612, 1995.
- Tsyganenko, N.A., Effects of the solar wind conditions on the global magnetospheric configuration as deduced from data-based models, in *Proceedings of ICS-3 Conference on Substorms, Versailles, France, Eur. Space Agency Spec. Publ., ESA SP-389*, 181-185, 1996.
- Voronkov, I., E. Friedrich, and J.C. Samson, Dynamics of the Substorm Growth Phase as Observed Using CANOPUS and SuperDARN Instruments, *J. Geophys. Res.*, *104*, 28,491-28,505, 1999.
- Zelenyi, L., A. Galeev, and C.F. Kennel, Ion precipitation from the inner plasma sheet due to stochastic diffusion, *J. Geophys. Res.*, *95*, 3871-3882, 1990.
- Zwingmann, W., Self-consistent magnetotail theory: Equilibrium structures including arbitrary variation along the tail axis, *J. Geophys. Res.*, *88*, 9101-9108, 1983.

---

E. Friedrich, J. C. Samson, and J. A. Wanliss, Department of Physics, University of Alberta, Edmonton, T6G 2J1, Canada. (wanliss@space.ualberta.ca)

(Received May 18, 2000; revised July 24, 2000; accepted August 7, 2000.)